METHODS

Ethical review

The protocol of this retrospective study was approved by the ethics committee of Yamanashi University Hospital, which waived the requirement for written informed consent because the study was a retrospective data analysis, with appropriate consideration given to patient risk, privacy, welfare, and rights.

Patients

We recruited 559 consecutive outpatients with chronic hepatitis B virus (HBV) or hepatitis C virus (HCV) infection who underwent gadoxetic acid-enhanced MRI at Yamanashi University Hospital between January 2008 and December 2010. The exclusion criteria were as follows: 1) presence or history of typical HCC (n = 420), because intrahepatic metastasis does not always develop through the usual multistep hepatocarcinogenesis process, skipping the early pathological stage with hypovascularity to an advanced pathological stage even when the size is small (16, 17); 2) Child-Pugh class C disease (n = 9), because the hepatocyte phase findings are not reliable in patients with this condition because of reduced gadoxetic acid uptake in the liver (18); and 3) patients who dropped out during the 3-year follow-up period (n = 3).

After excluding 432 patients, 127 patients were included in this retrospective cohort study. They were divided into groups with hypovascular nodules determined on the arterial phase and hypointensity on the hepatocyte phase (non-clean liver group; n = 18 patients) and without such nodules (clean liver group; n = 109 patients) as shown in Figure 1. In this study, we divided cases into two groups according to the presence or

absence of these nodules at the baseline, even when such nodules were initially detected during the follow-up period; we assigned these patients to the clean liver group.

Follow-up and diagnosis of HCC

All 127 patients were followed-up at the liver disease outpatient clinic of our institution with blood tests, including those for tumor markers, and diagnostic imaging modality (US, CT or MRI). The development of typical HCC that required treatment as proposed by the American Association for the Study of Liver Diseases (AASLD) guidelines (19) and that was diagnosed according to imaging criteria, showing arterial hypervascularity and venous phase washout, or based on histological examination of liver biopsies from hypovascular nodules that grew to >10 mm during follow-up. Biopsies were obtained using a 21-gauge core needle. Two patients each had a liver nodule >10 mm in diameter on initial MRI (12mm and 13mm), was diagnosed on the basis of the biopsy as a dysplastic nodule.

The endpoint of this study was the development of typical HCC not only from the hypovascular hypointense nodules observed initially but also from other areas without these nodules ("*de novo* HCC"). Dynamic CT and/or MRI were also performed in cases with hepatic nodules detected by US, liver cirrhosis, a tendency of tumor marker elevation, and difficult evaluation of the liver parenchyma by US. All the 127 patients were followed-up for 3 years after the initial gadoxetic acid-enhanced MRI examination. When imaging modalities led to diagnosis of HCC, recognizing hypervascularization by more than one experienced radiologist and other imaging modalities was regarded as the time of diagnosis of HCC. When needle biopsy was performed to investigate nodules, the time of diagnosis of HCC was when the

pathologists and physicians examined pathological tissue and diagnosed as HCC.

MRI

MRI was performed using a superconducting magnet that operated at 1.5 Tesla (Sigma EXCITE HD; GE Medical Systems, Milwaukee, WI) and an 8-channel phased-array coil. First, we obtained fast spoiled gradient-echo T1-weighted images (T1WIs) with dual echo acquisition and respiratory-triggered fat-saturated fast spin-echo T2-weighted images (T2WIs). Dynamic fat-suppressed gradient-echo T1WIs were obtained using a three-dimensional (3D) acquisition sequence before (precontrast) and 20-30 s, 60 s, 2 min, 5 min, 10 min, and 20 min after the administration of gadoxetic acid (Primovist; Bayer Schering Pharma, Berlin, Germany). This contrast agent (0.025 mmol/kg body weight) was administered intravenously as a bolus at a rate of 1 mL/s through an intravenous cubital line (20–22 gauge) that was flushed with 20 mL saline from a power injector. The delay time for the arterial phase scan was adjusted according to a fluoroscopic triggering method (20). All images were acquired in the transverse plane. Sagittal plane T1WIs were also obtained during the hepatocyte phase at 20 min after the injection of the contrast agent.

Statistical analysis

All continuous values are expressed as median (range). Fischer's exact probability test was used for comparisons between categorical variable and the non-parametric Mann-Whitney test was used to compare differences between continuous variables. Baseline clinical characteristics, including blood test results, were evaluated within 1 month of the initial MRI. We investigated whether or not HCC development was

associated with age, gender, fibrosis, etiology (HBV or HCV), platelet count, serum alanine aminotransferase (ALT), γ-glutamyl transpeptidase (γ-GTP), alpha-fetoprotein (AFP), and the presence or absence of hypovascular hypointense nodules.

Cumulative HCC development was estimated according to the Kaplan-Meier method and differences in the curves were tested using the log-rank test. Risk factors for HCC development were determined according to the Cox proportional hazard model. Subgroup analyses with a Cox proportional hazard model were applied to estimation of the hazard ratio (HR) of the non-clean liver group versus clean liver group in the dichotomized subgroups. All statistical analyses were performed using JMP software, version 10 (SAS Institute Japan, Tokyo, Japan). A two-sided p value <0.05 was considered statistically significant.

RESULTS

Characteristics of the patients and nodules

A total of 127 patients were enrolled, of whom 26 had chronic HBV infections and 101 had HCV infections, and 68 had virus-associated cirrhosis. No statistically significant differences in the initial clinical characteristics were found between the non-clean liver and clean liver groups (Table 1). Thirty five hypovascular hypointense nodules were found in 18 patients in the non-clean liver group (1–5 nodules per patient) at baseline (data not shown). Twenty-four of these 35 nodules were detectable only on the hepatocyte phase MRI and were undetectable by US, CT and non-hepatocyte phase MRI. None of the 35 nodules showed high intensity on T2WIs. The median nodule diameter was 8 mm (range: 4–13 mm, 33 nodules with 10mm or less, 2 nodules with 12 mm and 13 mm).

HCC incidence according to initial MRI findings

HCC was diagnosed in 17 patients, 10 in the non-clean liver group and 7 in the clean liver group; 14 of these patients had HCV infection. Thirteen patients were diagnosed according to the AASLD imaging criteria (19). Four patients were diagnosed pathologically by liver biopsies that were performed, based on enlargement of the nodules of >10 mm in diameter during the observation period.

The cumulative 1-, 2-, and 3-year HCC incidence rates were 1.5%, 10.2%, and 13.4%. As determined by the Kaplan-Meier method, these rates were 11.1% (95% confidence interval [CI], 0.0-25.6%), 38.8% (95% CI, 16.3-61.4%), and 55.5% (95% CI, 32.6-78.5%) in the non-clean liver group and 0.0% (95% CI, 0.0-2.3%), 5.5% (95%

CI, 0.0-9.8%), and 6.4% (95% CI, 1.8-11.0%) in the clean liver group; the former group showed significantly higher rates of development of typical HCC than the latter ($p < 0.001$) as shown in Figure 2. The median imaging intervals were 3 months (3-6 months) in the non-clean liver group and 4 months (2-12 months) in the clean liver group. The imaging interval of the non-clean liver group was shorter than clean liver group (3 vs. 4 months: $p = 0.015$). The median intervals between the initial MRI and HCC diagnosis was 16 months (9-32 months) in the non-clean liver group and 21 months (16-35 months) in the clean liver group.

In 11 of 17 patients with HCC development, HCCs developed at sites in which no nodules had been seen on the initial gadoxetic acid-enhanced MRI, *i.e. "de novo* HCC". These HCCs were found 4 in 18 patients in the non-clean liver group (3-year HCC incidence rates: 22.2%, 95% CI, 4.3-51.0%) and 7 in 109 patients in the clean liver group (3-year HCC incidence rates: 6.4%, 95% CI, 1.8-11.0%). The incidence rates of "*de novo* HCC" was significantly higher in the non-clean liver group than the clean liver group ($p = 0.003$, Figure 3). In the remaining 6 patients, HCCs developed at the same site of the initial nodules exclusively in 18 patients of a non-clean liver group by definition, and those HCCs arose among the nodules ≥8 mm in the initial MRI study.

Risk factors for HCC development

Univariate analyses showed that the significant risk factors for HCC development included older age ($p = 0.039$), cirrhosis ($p = 0.009$), a low platelet count ($p = 0.003$), a high AFP concentration ($p = 0.006$), and a non-clean liver ($p < 0.001$). Multivariate analysis with these variables revealed that older age (HR: 1.08; 95% CI, 1.01–1.16: $p = 0.024$), a low platelet count (HR 1.17; 95% CI, 1.03–1.35: $p = 0.017$), and a non-clean

liver (HR 9.41; 95% CI, 3.47–25.46: $p < 0.001$) were the only independent risk factors for HCC development (Table 2).

We further assessed the effect of a non-clean liver on the risk of HCC development in subgroups of these patients (Fig. 4). We found that belonging to the non-clean liver group was a significant risk factor in patients without HBV. Notably, this designation was particularly valuable for patients who are generally regarded as at low risk for HCC development: those without cirrhosis (HR 37.23; 95% CI, 3.30–419.71: $p = 0.003$) and those with high platelet counts (HR 33.42; 95% CI, 6.69–166.94: $p < 0.001$).

DISCUSSION

This study revealed presence of hypovascular hypointense liver nodules (non-clean liver) on gadoxetic acid-enhanced MRI, is a significant risk factor for subsequent development of typical HCC not only at the same sites but also at the different sites from the initial nodules. The incidence of development of typical HCC in the non-clean liver patients was >50% during a 3-year follow-up period, indicating these higher-risk patients should be rigorously investigated for the early detection of HCC during follow-up.

In the present study, 6 of the 18 patients in the non-clean liver group developed typical HCCs at the same site of the initial nodules during the subsequent 3 years (11.1%/year). Most of the hypovascular hypointense nodules on gadoxetic acid–enhanced MRI are considered precursor lesions of typical HCCs, such as early HCCs or high-grade dysplastic nodules, on histological examination (13-15), while it has been reported that most hypovascular nodules exhibiting high- to iso-intensity signals in the hepatocyte phase are benign hepatic nodules (14, 15). Recent studies have suggested that a reduction of OATP 1B3 (OATP 8) transporter expression begins at the earliest stage of hepatocarcinogenesis (21, 22), before changes in vascularity such as decreased portal flow or increased arterial flow. The progression rate of the small hypovascular hypointense nodules to typical HCC was reported as 10-17% / year (9, 10), which is comparable to the present study. Typical HCCs arose exclusively among the nodules ≥8 mm, as in previous studies that the larger size of the hypovascular hypointense nodules is the risk factor for progression to typical HCCs in the initial MRI study (9, 10).

Hyperintensity on T2WIs (12) or diffusion-weighted images (DWIs) (11) also was reported to be useful for prediction of typical HCC progress in hypovascular hypointense nodules. In our patients, none of the nodules in the non-clean liver group showed hyperintensity on T2WIs, suggesting that the hepatocyte phase is more sensitive for detecting the early-stage of hepatocarcinogenesis (15). DWIs were not evaluated in this study because this usually detects pathologically advanced HCCs of larger size or with hypervascularity (23). Thus, it is reasonable that the hepatocyte phase can effectively recognize the earliest stage of HCC development without T2WIs or DWIs.

In 11 of 17 patients, typical HCCs developed at sites other than the initially detected hypovascular hypointense nodules. As shown in Figure 3, the incidence rates of such HCCs in the non-clean liver group was significantly higher than in the clean liver group ($p = 0.003$), indicating a non-clean liver itself is a risk factor for HCC development, apart from the detectable hypovascular hypointense nodules. In addition, 4 patients with nodules even below 8mm, 2 patients developed HCC at different sites from the initial nodules during follow up (data not shown). Taken together, a liver with non-clean liver has the higher potential for hepatocarcinogenesis or for undetectable precursor lesions. The non-clean liver might reflect more advanced genetic or epigenetic changes in the background hepatocytes, however, the detailed biological mechanism is not clear in this study.

Non-clean liver was an independent risk factor for the development of typical HCC, apart from well-documented risk factors (Table 2), such as cirrhosis (24), ALT (25), γ-GTP (26), age and AFP (27). A non-clean liver is a significant risk for HCC development also for those without cirrhosis or with high platelet counts (Figure 4). This means patients at more increased risk of HCC development can be discerned as a

non-clean liver even among low-risk subgroups.

Conversely, patients without such nodules (clean liver group) showed a significantly lower risk of developing typical HCC than those with non-clean livers (0.0% vs. 11.1% in 1-year, 6.8% vs. 55.5% at 3-years follow-up; $p < 0.001$), suggesting that gadoxetic acid-enhanced MRI could detect precursor lesions sensitively enough to rule out immediate (within 1 year) development of typical HCC. Although 7 patients in the clean liver group developed typical HCCs only after 1 year, these patients had other risk factors for HCC development, including lower platelet counts, implying more advanced liver cirrhosis, or high AFP (data not shown). Such HCCs might arise from precursor lesions that cannot be visualized by current imaging techniques.

This study is a retrospective study and has some limitations. We included patients with HBV and HCV together, because gadoxetic acid-enhanced MRI findings or HCC development do not differ between these two groups and HBV or HCV infection is not an independent risk factor for typical HCC development. However, the number of HBV patients was too small ($n = 26$) to statistically confirm the current result when limited to HBV patients only. Prospective studies with larger numbers of patients who have uniform liver disease etiologies and imaging intervals are needed to verify our findings in different settings. Although the imaging interval of the non-clean liver group was shorter than the clean liver group (3 vs. 4 months: $p = 0.015$), the median intervals between the initial MRI and HCC diagnosis was 16 months in the non-clean liver group and 21 months in the clean liver group. They are short enough for cumulative detection of HCC development for three years and it is assumed that there was little influence on the conclusions.

In conclusion, patients with chronic viral liver disease are at high risk for

developing typical HCCs at any sites of the liver if they have hypovascular hypointense nodules on gadoxetic acid-enhanced MRI. These patients should be closely followed up for developing typical HCC not only at the same site but also at the different sites from the initial nodule.

REFERENCES

1. Ichikawa T, Saito K, Yoshioka N, Tanimoto A, Gokan T, Takehara Y, et al. Detection and characterization of focal liver lesions: A Japanese phase III, multicenter comparison between gadoxetic acid disodium-enhanced magnetic resonance imaging and contrast-enhanced computed tomography predominantly in patients with hepatocellular carcinoma and chronic liver disease. Invest Radiol. 2010;45(3):133-41.
2. Halavaara J, Breuer J, Ayuso C, Balzer T, Bellin MF, Blomqvist L, et al. Liver tumor characterization: comparison between liver-specific gadoxetic acid disodium-enhanced MRI and biphasic CT--a multicenter trial. J Comput Assist Tomogr. 2006;30(3):345-54.
3. Hamm B, Staks T, Muhler A, Bollow M, Taupitz M, Frenzel T, et al. Phase I clinical evaluation of Gd-EOB-DTPA as a hepatobiliary MR contrast agent: safety, pharmacokinetics, and MR imaging. Radiology. 1995;195(3):785-92.
4. Hammerstingl R, Huppertz A, Breuer J, Balzer T, Blakeborough A, Carter R, et al. European EOB-study group. Diagnostic efficacy of gadoxetic acid (Primovist)-enhanced MRI and spiral CT for a therapeutic strategy: comparison with intraoperative and histopathologic findings in focal liver lesions. Eur Radiol. 2008;18(3):457-67.
5. Huppertz A, Balzer T, Blakeborough A, Breuer J, Giovagnoni A, Heinz-Peer G, et al. European EOB Study Group. Improved detection of focal liver lesions at MR imaging: multicenter comparison of gadoxetic acid-enhanced MR images with intraoperative findings. Radiology. 2004;230(1):266-75.

6. Di Martino M, Marin D, Guerrisi A, Baski M, Galati F, Rossi M, et al. Intraindividual comparison of gadoxetate disodium-enhanced MR imaging and 64-section multidetector CT in the detection of hepatocellular carcinoma in patients with cirrhosis. Radiology. 2010;256(3):806-16.

7. Inoue T, Kudo M, Komuta M, Hayaishi S, Ueda T, Takita M, et al. Assessment of Gd-EOB-DTPA-enhanced MRI for HCC and dysplastic nodules and comparison of detection sensitivity versus MDCT. J Gastroenterol. 2012;47(9):1036-47.

8. Golfieri R, Renzulli M, Lucidi V, Corcioni B, Trevisani F, Bolondi L. Contribution of the hepatobiliary phase of Gd-EOB-DTPA-enhanced MRI to dynamic MRI in the detection of hypovascular small (</= 2 cm) HCC in cirrhosis. Eur Radiol. 2011;21(6):1233-42.

9. Kumada T, Toyoda H, Tada T, Sone Y, Fujimori M, Ogawa S, et al. Evolution of hypointense hepatocellular nodules observed only in the hepatobiliary phase of gadoxetate disodium-enhanced MRI. AJR Am J Roentgenol. 2011;197(1):58-63.

10. Motosugi U, Ichikawa T, Sano K, Sou H, Onohara K, Muhi A, et al. Outcome of hypovascular hepatic nodules revealing no gadoxetic acid uptake in patients with chronic liver disease. J Magn Reson Imaging. 2011;34(1):88-94.

11. Kim YK, Lee WJ, Park MJ, Kim SH, Rhim H, Choi D. Hypovascular hypointense nodules on hepatobiliary phase gadoxetic acid-enhanced MR images in patients with cirrhosis: Potential of DW imaging in predicting progression to hypervascular HCC. Radiology. 2012;265(1):104-14.

12. Hyodo T, Murakami T, Imai Y, Okada M, Hori M, Kagawa Y, et al. Hypovascular nodules in patients with chronic liver disease: risk factors for development of hypervascular hepatocellular carcinoma. Radiology. 2013;266(2):480-90.

13. Bartolozzi C, Battaglia V, Bargellini I, Bozzi E, Campani D, Pollina LE, et al. Contrast-enhanced magnetic resonance imaging of 102 nodules in cirrhosis: correlation with histological findings on explanted livers. Abdom Imaging. 2013;38(2):290-6.

14. Golfieri R, Grazioli L, Orlando E, Dormi A, Lucidi V, Corcioni B, et al. Which is the best MRI marker of malignancy for atypical cirrhotic nodules: hypointensity in hepatobiliary phase alone or combined with other features? Classification after Gd-EOB-DTPA administration. J Magn Reson Imaging. 2012;36(3):648-57.

15. Sano K, Ichikawa T, Motosugi U, Sou H, Muhi AM, Matsuda M, et al. Imaging study of early hepatocellular carcinoma: usefulness of gadoxetic acid-enhanced MR imaging. Radiology. 2011;261(3):834-44.

16. Motosugi U. Hypovascular hypointense nodules on hepatocyte phase gadoxetic acid-enhanced MR images: Too early or too progressed to determine hypervascularity. Radiology. 2013;267(1):317-8.

17. Asayama Y, Yoshimitsu K, Nishihara Y, Irie H, Aishima S, Taketomi A, et al. Arterial blood supply of hepatocellular carcinoma and histologic grading: radiologic-pathologic correlation. AJR Am J Roentgenol. 2008;190(1):W28-34.

18. Motosugi U, Ichikawa T, Sou H, Sano K, Tominaga L, Kitamura T, et al. Liver parenchymal enhancement of hepatocyte-phase images in Gd-EOB-DTPA-enhanced MR imaging: which biological markers of the liver function affect the enhancement? J Magn Reson Imaging. 2009;30(5):1042-6.

19. Bruix J, Sherman M. American Association for the Study of Liver Diseases. Management of hepatocellular carcinoma: an update. Hepatology. 2011;53(3):1020-2.

20. Motosugi U, Ichikawa T, Araki T. Rules, roles, and room for discussion in gadoxetic acid-enhanced magnetic resonance liver imaging: current knowledge and future challenges. Magnetic Rsonance in Medical Sciences. 2013;12(3):161-75.

21. Kitao A, Zen Y, Matsui O, Gabata T, Kobayashi S, Koda W, et al. Hepatocellular carcinoma: signal intensity at gadoxetic acid-enhanced MR Imaging--correlation with molecular transporters and histopathologic features. Radiology. 2010;256(3):817-26.

22. Narita M, Hatano E, Arizono S, Miyagawa-Hayashino A, Isoda H, Kitamura K, et al. Expression of OATP1B3 determines uptake of Gd-EOB-DTPA in hepatocellular carcinoma. J Gastroenterol. 2009;44(7):793-8.

23. Nasu K, Kuroki Y, Tsukamoto T, Nakajima H, Mori K, Minami M. Diffusion-weighted imaging of surgically resected hepatocellular carcinoma: imaging characteristics and relationship among signal intensity, apparent diffusion coefficient, and histopathologic grade. American Journal of Roentgenology. 2009;193(2):438-44.

24. Degos F, Christidis C, Ganne-Carrie N, Farmachidi JP, Degott C, Guettier C, et al. Hepatitis C virus related cirrhosis: time to occurrence of hepatocellular carcinoma and death. Gut. 2000;47(1):131-6.

25. Tarao K, Rino Y, Ohkawa S, Shimizu A, Tamai S, Miyakawa K, et al. Association between high serum alanine aminotransferase levels and more rapid development and higher rates of incidence of hepatocellular carcinoma in patients with hepatitis C virus-associated cirrhosis. Cancer. 1999;86(4):589-95.

26. Ikeda K, Saitoh S, Suzuki Y, Kobayashi M, Tsubota A, Koida I, et al. Disease

progression and hepatocellular carcinogenesis in patients with chronic viral hepatitis: a prospective observation of 2215 patients. J Hepatol. 1998;28(6):930-8.

27. Ikeda K, Saitoh S, Koida I, Arase Y, Tsubota A, Chayama K, et al. A multivariate analysis of risk factors for hepatocellular carcinogenesis: a prospective observation of 795 patients with viral and alcoholic cirrhosis. Hepatology. 1993;18(1):47-53.

FIGURE LEGENDS

Figure 1. Patient inclusion criteria. "*De novo* HCC" is a typical HCC that developed at sites in which no nodules had been seen on the initial gadoxetic acid-enhanced MRI.

Figure 2. Cumulative incidence rates of typical HCC development in the non-clean and clean liver groups.

Figure 3. Cumulative incidence rates of typical HCC at sites in which no nodules had been seen on the initial gadoxetic acid-enhanced MRI, *i.e.* "*de novo* HCC".

Figure 4. Stratified analyses of the non-clean liver as a risk factor for typical HCC development.

Table 1. Baseline patient characteristics.

Characteristics	Total n = 127	Non-clean liver n = 18	Clean liver n = 109	p value
Age in years	65 (30-88)	68 (46-82)	64 (30-88)	0.15
Male/female	68/59	10/8	58/51	1.00
Non-cirrhosis/cirrhosis	59/68	6/12	53/56	0.31
HBV/HCV	26/101	5/13	21/88	0.53
Platelet count ($x10^9$/L)	122 (30-410)	102 (46-187)	125 (30-410)	0.07
ALT (IU/L)	32 (7-206)	32 (14-95)	32 (7-206)	0.97
γ-GTP (IU/L)	31 (9-305)	31 (13-258)	31 (9-305)	0.68
AFP (ng/mL)	4 (1-582)	8 (2-181)	4 (1-582)	0.19

Note: Continuous data are shown as medians (range).

Table 2. Variables that predict HCC development: univariate and multivariate analyses.

	Univariate		Multivariate	
Variables	Hazard ratio (95% CI)	p value	Hazard ratio (95% CI)	p value
Male	0.56 (0.29-1.95)	0.755		
Age (per year)	1.06 (1.00-1.12)	0.039	1.08 (1.01-1.16)	0.024
Cirrhosis	14.37 (1.90-108.44)	0.009	3.54 (0.37-33.77)	0.231
HCV (vs. HBV)	4.39 (0.58-33.17)	0.151		
Platelet count (per 10^{10}/L)	1.19 (1.06-1.33)	0.003	1.17 (1.03-1.35)	0.017
ALT (per IU/L)	1.00 (0.99-1.02)	0.423		
γ-GTP (per IU/L)	1.00 (0.99-1.01)	0.688		
AFP > 10 ng/mL	3.98 (1.47-10.77)	0.006	1.47 (0.49-4.33)	0.486
Non-clean liver	12.36 (4.68-32.61)	< 0.001	9.41 (3.47-25.46)	< 0.001

Fig. 1

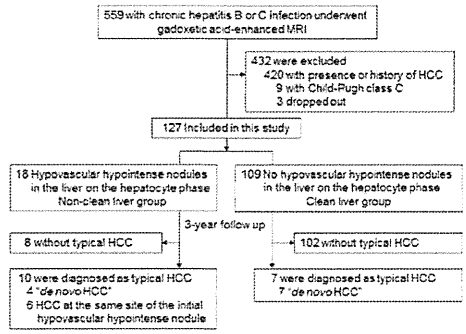

hepr_12309_f1

Fig. 2

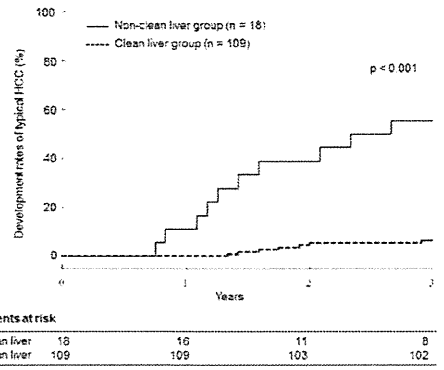

No. of patients at risk

Non-Clean liver	18	16	11	8
Clean liver	109	109	103	102

hepr_12309_f2